HHS Public Access

Author manuscript

Cell Rep. Author manuscript; available in PMC 2016 January 13.

Published in final edited form as:

Cell Rep. 2015 January 13; 10(2): 266–279. doi:10.1016/j.celrep.2014.12.023.

Adipose fatty acid oxidation is required for thermogenesis and potentiates oxidative stress induced inflammation

Jieun Lee[1], **Jessica M. Ellis**[1,2], and **Michael J. Wolfgang**[1,*]

[1]Department of Biological Chemistry, Center for Metabolism and Obesity Research, Johns Hopkins University School of Medicine, Baltimore, Maryland 21205

SUMMARY

To understand the contribution of adipose tissue fatty acid oxidation to whole-body metabolism, we generated mice with an adipose specific knockout of Carnitine Palmitoyltransferase 2 ($CPT2^{A-/-}$), an obligate step in mitochondrial long chain fatty acid oxidation. $CPT2^{A-/-}$ mice became hypothermic after an acute cold challenge and $CPT2^{A-/-}$ brown adipose tissue (BAT) failed to up-regulate thermogenic genes in response to agonist-induced stimulation. The adipose-specific loss of CPT2 resulted in diet-dependent changes in adiposity but did not result in changes in body weight on low or high fat diets. Additionally, $CPT2^{A-/-}$ mice had suppressed high fat diet induced oxidative stress and inflammation in visceral white adipose tissue (WAT), however, high fat diet-induced glucose intolerance was not improved. These data show that fatty acid oxidation is required for cold-induced thermogenesis in BAT and high fat diet induced oxidative stress and inflammation in WAT.

INTRODUCTION

Ingestion of a calorically dense diet, generally high in fat content, coupled with inactivity leads to increased adiposity and eventual obesity. Obesity in turn is highly correlated with the development of type 2 diabetes, the metabolic syndrome, and cardiovascular disease among others. The molecular mechanisms by which high fat diets contribute to these pathologies are not well understood, but several themes have emerged. Implicated in the etiology and progression of obesity related pathologies is oxidative stress, ER-stress, and inflammation originating locally at adipose depots but acting systemically to promote insulin resistance (Glass and Olefsky, 2012; Hotamisligil, 2010; Keaney et al., 2003; Kusminski

*Address correspondence to: Michael J. Wolfgang, Ph.D, Department of Biological Chemistry, Johns Hopkins University School of Medicine, 855 N. Wolfe St., 475 Rangos Building, Baltimore, MD 21205, Tel: 443-287-7680, mwolfga1@jhmi.edu.
[2]Current address: Jessica M. Ellis, Ph.D, Department of Nutrition Science, Purdue University, West Lafayette, Indiana 47907. jmellis@purdue.edu

Conflict of Interest

The authors have no competing financial interests.

Author Contributions

J.L., J.M.E. and M.J.W. performed experiments and wrote the manuscript.

and Scherer, 2012). Reversing or preventing local adipose tissue inflammation may have beneficial systemic effects against insulin resistance. Alternatively, strategies to reverse obesity by increasing adipose energy expenditure have been suggested to improve systemic obesity-related complications (Tseng et al., 2010).

Adult mammals have at least two functionally distinct adipose lineages, unilocular white adipocytes which function mainly to store fat and multilocular brown adipocytes which function mainly to burn fat for thermogenesis. Dysfunctional WAT and BAT have been implicated in the pathogenesis of obesity and diabetes. BAT is densely packed with mitochondria and require fatty acid oxidation to fuel heat generation (Ellis et al., 2010; Guerra et al., 1998; Ji et al., 2008; Schuler et al., 2005; Tolwani et al., 2005). Although the oxidation of fatty acids in WAT in the fed state is relatively low, fasting doubles the rate of white adipocyte fatty acid oxidation and is presumably a major fuel in insulin suppressed states (Wang et al., 2003). Changing macronutrient metabolism specifically in adipocytes can lead to changes in adiposity, body weight and glucose tolerance (Abel et al., 2001; Ahmadian et al., 2011; Lodhi et al., 2012; Vernochet et al., 2012). However, the autonomous contribution of adipose fatty acid oxidation to obesity and insulin resistance remains unknown.

Mitochondrial long chain fatty acid beta-oxidation requires successive carnitine acyltransferases to translocate acyl-CoAs from the cytoplasm into the mitochondrial matrix (Wolfgang and Lane, 2006). The initial and rate setting enzyme, CPT1, generates acyl-carnitines that can traverse the mitochondrial membranes via specific transporters. CPT1 is allosterically inhibited by the rate determining metabolite in *de novo* fatty acid synthesis, malonyl-CoA; therefore, the balance of fatty acid synthesis and oxidation is metabolically coordinated post-translationally. Once inside the mitochondrial matrix, CPT2 generates acyl-CoAs from acyl-carnitines to initiate the beta-oxidation of long chain fatty acids to acetyl-CoA. Fatty acids contain an abundant energy potential making them ideal for storage during energy surplus and mobilization during energy deficits. Fatty acid oxidation efficiently generates energy but can also promote the generation of reactive oxygen species (ROS). ROS can potentiate oxidative stress and inflammation, which can impair insulin sensitivity (Houstis et al., 2006).

Although it is clear that fatty acid oxidation is a critical and fundamental metabolic end point in humans (Longo et al., 2006) and rodents (Ji et al., 2008; Nyman et al., 2005), it is not clear how adipocyte fatty acid oxidation affects whole-body metabolism in an autonomous manner. Therefore, we generated a conditional loss-of-function allele for CPT2, an obligate step in mitochondrial long chain fatty acid beta-oxidation that is encoded by a single gene. Here we show that adipose tissue fatty acid oxidation is not only required for acute cold adaptation, but also for the induction of thermogenic genes in BAT. The loss of adipose fatty acid oxidation altered adiposity in a diet dependent manner but did not lead to diet-induced changes in body weight. Furthermore, we show that in white adipose tissue, the loss of fatty acid oxidation reduces high fat induced oxidative stress and inflammation but does not alter the progression of obesity or glucose intolerance.

RESULTS

Generation of mice with an adipose tissue specific deletion of CPT2

Mitochondrial long chain fatty acid oxidation requires sequential carnitine acyltransferases to translocate acyl-CoAs into the mitochondrial matrix. The regulated and rate setting enzyme, CPT1, is encoded by multiple isoenzymes that can functionally compensate in some tissues (Haynie et al., 2013). Therefore, to generate a mouse model to assess the tissue specific roles and requirements of fatty acid oxidation, we generated a conditional loss-of-function allele for CPT2, an enzyme required in mitochondrial long chain fatty acid beta-oxidation that is encoded by a single gene. C57BL/6 embryonic stem cells were used to target loxP recombination sites surrounding Exon 4 of the *Cpt2* gene (Fig. 1A). Exon 4 encompasses ~1/3 of the protein coding sequence including all of the critical catalytic residues (Hsiao et al., 2006). Loss of exon 4 is predicted to additionally cause a frame-shift in the remaining exons. To produce mice with a loss of CPT2 specifically in adipocytes, we bred $CPT2^{lox/lox}$ mice to adipocyte specific Adiponectin-Cre transgenic mice (Eguchi et al., 2011). The resulting adipose specific CPT2 KO mice, $CPT2^{A-/-}$, have a loss of *Cpt2* mRNA in all adipose depots examined (Fig. 1B). Furthermore, CPT2 protein is substantially reduced in brown adipose tissue of $CPT2^{A-/-}$ mice (Fig. 1C). As expected, *ex vivo* gWAT, iWAT and BAT explants derived from $CPT2^{A-/-}$ mice had a greatly suppressed ability to oxidize radiolabeled 1-^{14}C-oleic acid (Fig. 1D). Long chain mitochondrial fatty acid beta-oxidation can not proceed in the absence of CPT2. The remaining oxidation of oleic acid in tissues was presumably due to either peroxisomal fatty acid oxidation or oxidation in non-parenchymal cells within the adipose depots. To test this directly, we derived and immortalized mouse embryonic fibroblasts (MEFs) from $CPT2^{lox/lox}$ embryos and infected them with a control or Cre recombinase expressing virus. The oxidation of 1-^{14}C-oleic acid in $CPT2^{lox/lox}$ MEFs was severely blunted by incubating cells with a large dose (100uM) of the mitochondrial fatty acid oxidation inhibitor etomoxir. The genetic loss of CPT2 in MEFs suppressed oleic acid oxidation to the same degree as etomoxir (Fig. 1E). However, the oxidation of the very long chain lignoceric acid (C24:0), which is oxidized mainly in peroxisomes, was not significantly changed (Fig. 1E). Therefore, the deletion of CPT2 represents an effective strategy for inhibiting long chain mitochondrial fatty acid beta-oxidation.

To determine how the loss of CPT2 alters white adipose fatty acid oxidative metabolites, we measured the steady-state concentration of carnitine and acyl-carnitine species in iWAT of control and $CPT2^{A-/-}$ mice. Although CPT2 deficiency results in the inability to utilize long chain acyl-carnitines and people with CPT2 mutations are diagnosed by the elevation of these metabolites in serum, $CPT2^{A-/-}$ mice did not have increased long chain acyl-carnitine species in iWAT. Instead, $CPT2^{A-/-}$ iWAT had a strong trend towards suppressed free carnitine and acetyl-carnitine and statistically significant reductions in several short chain acyl-carnitines (Fig. 1F). We conclude that long chain acyl-carnitines do not build up in WAT but are readily transported out of the adipocyte resulting in a tissue specific carnitine deficiency due to the inability to properly recycle carnitine in $CPT2^{A-/-}$ WAT. In summary, we have generated mice with an adipose-specific defect in mitochondrial long chain fatty

acid oxidation that is mediated by the loss of an obligate non-compensatory step in fatty acid oxidation.

Adipose fatty acid oxidation is required for cold induced thermogenesis

Brown adipose tissue is essential for heat generation during an acute cold exposure in perinatal and adult mammals (Kozak, 2010; Lowell et al., 1993; Tseng et al., 2010). The requirement of fatty acid oxidation during cold thermogenesis is made evident by cold intolerant phenotypes of whole body knockout mouse models of the acyl-CoA dehydrogenase enzymes (Guerra et al., 1998; Schuler et al., 2005; Tolwani et al., 2005). To determine the autonomous requirement of adipose fatty acid oxidation during adaptive thermogenesis, we placed 12 week old control and $CPT2^{A-/-}$ female mice at 4°C and measured their body temperature over 3 hours. Although all of the mice visibly shivered, cold intolerance was evident in $CPT2^{A-/-}$ mice, reaching critical hypothermia (30°C) within 3 hours (Fig. 2A). The body weights of 12 week old female $CPT2^{A-/-}$ mice were not different (Fig. 2B). Upon dissection, $CPT2^{A-/-}$ interscapular BAT was visibly lipid laden, displaying a milky appearance in contrast to the dark brown color of control BAT (Fig. 2C). Histologic evaluation demonstrated increased lipid droplet accumulation that did not dissipate upon cold stimulation (Fig. 2D). Consistent with these morphologic changes, cold exposed $CPT2^{A-/-}$ BAT maintained ~3-fold increase in triglyceride content compared to BAT from control mice (Fig. 2E). Evaluation of serum metabolites showed normal responses of serum glucose, ketone bodies and triglycerides to cold stimulation in $CPT2^{A-/-}$ mice. However, compared to controls, $CPT2^{A-/-}$ mice had increased serum free fatty acids and decreased glycerol during cold stimulation, likely due to their inability to utilize the mobilized fatty acids in CPT2 null BAT (Fig. 2F). These data show that adipose fatty acid oxidation is required for acute cold induced thermogenesis.

BAT fatty acid oxidation is required for agonist induced thermogenic gene expression

To understand the transcriptional control of BAT metabolism in $CPT2^{A-/-}$ mice, we determined the expression of fatty acid catabolic and anabolic genes. After a 3hr cold stimulation the fatty acid oxidative genes *Acox1*, *Cpt1b* and *Lcad* were suppressed in $CPT2^{A-/-}$ BAT (Fig. 3A). Malonyl-CoA decarboxylase (*Mlycd*), which decarboxylates malonyl-CoA and therefore dysinhibits CPT1, was greatly suppressed in both basal and cold stimulated $CPT2^{A-/-}$ BAT. Additionally, fatty acid biosynthetic genes *Pcx*, *Acaca* and *Elovl6*, were suppressed after a 3hr cold stimulation in $CPT2^{A-/-}$ BAT compared to controls (Fig. S1A). These data suggest that the loss of fatty acid oxidation in BAT feeds back to inhibit genes in fatty acid oxidation. To better understand the role of fatty acid oxidation on thermogenic programing in BAT, we measured the transcriptional response of BAT to cold stimulation. The canonical cold induced genes, *Ucp1*, *Pgc1*α, and *Dio2* were induced robustly in BAT of control mice after 3 hours at 4°C but were unresponsive in $CPT2^{A-/-}$ BAT (Fig. 3B). In fact, *Ucp1* and *Dio2* were suppressed constitutively even at room temperature. *Ucp1* and *Pgcl*α are thermogenic genes regulated by adrenergic signaling upon cold exposure. Therefore, we determined if $CPT2^{A-/-}$ BAT was responsive to adrenergic stimulation by injecting $CPT2^{A-/-}$ and control mice with the selective β3-adrenergic agonist, CL-316243 (10mg/kg) and collected BAT 3hrs later. Unlike the control, $CPT2^{A-/-}$ BAT

elicited no increase in the mRNA abundance of *Ucp1* or *Pgc1α* (Fig. 3B). This suggests a strong defect in CPT2$^{A-/-}$ BAT thermogenic gene expression.

To determine where in the adrenergic signaling pathway CPT2$^{A-/-}$ BAT was impaired, we collected control and CPT2$^{A-/-}$ BAT explants and stimulated them *ex vivo* with 10μM CL-316243, the β-adrenergic agonist isoproterenol, or the adenylyl cylase activator, forskolin, in the presence of 200uM fatty acids (2:1 oleate:palmitate). All of these activators robustly induced *Ucp1* in control explants, however, CPT2$^{A-/-}$ BAT was unable to induce *Ucp1* (Fig. 3C). These data suggest that the defect in cold induced thermogenic gene expression is mediated downstream of the adrenergic receptor.

To determine if CPT2$^{A-/-}$ BAT was activating signaling downstream of adrenergic stimulation, we probed for PKA targets of adrenergic signaling after a 30 min stimulation with 10mg/kg CL-316243 *in vivo*. Utilizing a PKA phosphorylated substrate specific antibody, both control and CPT2$^{A-/-}$ BAT showed robust CL-316243 mediated phosphorylation (Fig. 3D). Additionally, cAMP response element-binding protein (CREB) phosphorylation, the canonical transcription factor downstream of adrenergic stimulation, elicited a robust phosphorylation in both control and CPT2$^{A-/-}$ BAT (Fig. 3E). These data show that CPT2$^{A-/-}$ BAT can activate adrenergic signaling and phosphorylation of downstream targets such as CREB. This suggests the defect in agonist induced thermogenic gene expression is likely at the level of transcriptional regulation. Taken together, these experiments show that CPT2$^{A-/-}$ BAT is resistant to agonist induced thermogenic gene expression and further suggests that fatty acid oxidation in BAT is coupled to agonist-induced transcription.

CPT2$^{A-/-}$ mice are defective in environmental temperature adaptation

Mammals can dramatically alter their physiology to adapt to the ambient temperature. Cold acclimation of UCP1KO mice is sufficient to rescue their acute cold intolerance (Golozoubova et al., 2001; Ukropec et al., 2006). To test the role of adipose fatty acid oxidation on this adaptation, we cold acclimatized CPT2$^{A-/-}$ mice to 15°C and then subjected them to an acute 4°C cold challenge. At 15°C, CPT2$^{A-/-}$ and control mice had lower body temperatures (~35.5°C) that upon cold challenge initially rose rapidly. However, CPT2$^{A-/-}$ mice could not maintain body temperature and after 4 hrs reached critical hypothermia (Fig. 3F). Again, *Ucp1*, and *Dio2* mRNA abundance were suppressed in CPT2$^{A-/-}$ BAT (Fig. 3G). This suggests that adipose fatty acid oxidation has additional roles other than merely activating UCP1 in BAT. Next, we asked if the inhibition of agonist-induced thermogenic gene expression at 21°C and 15°C was due to tonic activation of thermogenic signaling and therefore constitutively inhibited via negative feedback. To eliminate tonic basal thermogenic signaling, we acclimatized CPT2$^{A-/-}$ and control mice to a thermoneutral environment (30°C). We then injected the mice with 10mg/kg CL-316243 or vehicle and collected BAT 3hrs later. Thermoneutral acclimatization did not improve agonist-induced thermogenic gene expression in CPT2$^{A-/-}$ mice. In fact, the difference between control and CPT2$^{A-/-}$ mice was further exacerbated suggesting that the transcriptional defect is not due to tonic inhibition but is a primary defect (Fig. 3H). These data show that adipose fatty acid oxidation is critical for thermal adaptation.

Loss of adipose fatty acid oxidation disrupts mitochondrial homeostasis in BAT

The lack of agonist induced *Pgc1*α expression, a gene key to mitochondrial biogenesis, prompted us to examine mitochondrial proteins and mitochondrial density in CPT2$^{A-/-}$ BAT. Several mitochondrial proteins were suppressed in CPT2$^{A-/-}$ BAT under basal (21°C) conditions including ACO2 and MCAD (Fig. 3I & Fig. S1). These changes were exacerbated after 3hrs of cold stimulation. To determine mitochondrial number we quantified BAT mitochondrial DNA and found that gWAT and iWAT maintained normal mitochondrial DNA content whereas CPT2$^{A-/-}$ BAT had about a 2-fold suppression in mitochondrial DNA (Fig. 3J). These data show that mitochondrial long chain fatty acid oxidation in BAT is important for cellular bioenergetics but also for nuclear encoded mitochondrial gene expression, mitochondrial protein abundance and density.

Bioenergetic contribution of adipose fatty acid oxidation

In the absence of cold stimulation, it was not clear what the contribution of adipose fatty acid oxidation is to whole body energy expenditure under standard physiological conditions or perturbations. To determine the physiological contributions of adipose fatty acid oxidation, we housed control and CPT2$^{A-/-}$ mice individually in metabolic cages and measured metabolic parameters continuously during *ad libitum* feeding and fasting conditions. Consistent with a requirement for fatty acid oxidation during cold exposure, an injection of CL-316243 rapidly increased oxygen consumption in control mice, but was completely ineffective in altering oxygen consumption in CPT2$^{A-/-}$ mice (Fig. 4A). Unlike other models where changes in fatty oxidation drive changes in feeding behavior (Abu-Elheiga et al., 2001), CPT2$^{A-/-}$ mice had no changes in food intake compared to control mice (Fig. 4B). Interestingly, CPT2$^{A-/-}$ mice consumed more water than controls during the course of the experiment, particularly during fasting (Fig. 4C). This suggests that adipose tissue fatty acid oxidation may play a role in the generation and balance of water, similar to the role of lipid oxidation during hibernation (Nelson et al., 1973). There were minor reductions in energy expenditure and increased respiratory exchange ratio in CPT2$^{A-/-}$ mice relative to controls (Fig. 4D,E). Additionally, there was a modest increase in ambulatory activity in CPT2$^{A-/-}$ mice that may reflect a compensatory requirement of energy expenditure from skeletal muscle (Fig. 4F). These data show that adipose fatty acid oxidation contributes to overall energy expenditure in the absence of cold stimulation albeit minimally.

Loss of adipose fatty acid oxidation results in diet dependent changes in adiposity but not body weight

It has been suggested that mitochondrial dysfunction and suppressed BAT or WAT fatty acid oxidation contributes to changes in body weight and glucose tolerance (Keaney et al., 2003; Kusminski and Scherer, 2012). CPT2$^{A-/-}$ BAT is both bioenergetically and transcriptionally unable to support thermogenesis. Additionally, we have shown that the oxidation of fatty acids in adipose tissue is not a major determinant of whole animal bioenergetics during *ad libitum* or fasting conditions. To determine the consequences of a chronic long term inability to oxidize fatty acids in adipocytes on body weight, we placed control and CPT2$^{A-/-}$ mice on matched low and high fat diets for 12 weeks and measured

their body weights weekly. CPT2$^{A-/-}$ mice elicited no change in body weight, compared to control littermates, fed either a high fat or low fat diet (Fig. 5A). Evaluation of fat and lean content revealed a 64% increase in fat mass in low fat fed CPT2$^{A-/-}$ mice (Fig. 5B,C). Measurement of fat pad weights of low fat fed CPT2$^{A-/-}$ mice showed 67% increases in both gonadal and inguinal fat pads (Fig. 5D). High fat fed CPT2$^{A-/-}$ mice displayed a suppression of fat mass that was mainly the result of changes in inguinal adiposity (Fig. 5C,D). These seemingly paradoxical results are actually consistent with other models with dysfunctional adipose fatty acid oxidation or uncoupling (Ellis et al., 2010; Liu et al., 2003), and likely reflect compensatory increases in energy expenditure in tissues other than adipose. The expression of fatty acid biosynthetic genes was largely unchanged between control and CPT2$^{A-/-}$ gWAT, however, there were increases in fatty acid oxidative genes *Cpt1a* and *Mlycd* in low fat fed CPT2$^{A-/-}$ gWAT (Fig. S2A). This suggests distinct regulatory mechanisms in CPT2$^{A-/-}$ BAT and gWAT since *Cpt1b* and *Mlycd* were decreased in CPT2$^{A-/-}$ BAT. Consistent with increased compensatory energy expenditure, high fat fed CPT2$^{A-/-}$ mice displayed about a 2-fold increase in circulating ketones compared to control high fat fed mice (Fig. 5E). Analysis of gene expression in iWAT and liver of control and CPT2$^{A-/-}$ mice show that under high fat conditions many of the changes between the geneotypes were concentrated in the iWAT (Fig. S2B). Conversely, liver from control and CPT2$^{A-/-}$ mice showed most differences after low fat feeding (Fig. S2C). This shows that individual tissues and even different adipose depots respond disparately. These data demonstrate that the loss of adipose fatty acid oxidation does not contribute to changes in total body weight regardless of dietary lipid content, but that CPT2$^{A-/-}$ mice displayed differences in adiposity that were diet dependent.

Loss of adipose fatty acid oxidation is compensated in part by altered carbohydrate metabolism

The diet dependent changes in adiposity in CPT2$^{A-/-}$ mice are consistent with other cold intolerant models (Ellis et al., 2010; Liu et al., 2003). Nonetheless, we were interested in determining the flux of macronutrients in tissues lacking CPT2. First we directly tested the ability of CPT2$^{A-/-}$ mice to fully oxidize radiolabeled 1-^{14}C oleic acid *in vivo*. Consistent with the indirect calorimetry data, we did not observe differences in whole body fatty acid oxidation between control and CPT2$^{A-/-}$ mice (Fig. S3). Next, we determined the rate of *de novo* fatty acid synthesis by injecting ^{3}H-acetate to control and CPT2$^{A-/-}$ mice for 3hrs and extracting lipids from liver, gWAT and BAT. Although the livers of control and CPT2$^{A-/-}$ mice had equal incorporation of ^{3}H-acetate into lipids, both gWAT and BAT had about a 2-fold increase in incorporation (Fig. 6A). This suggested that there was an increase in carbohydrate utilization in cells where CPT2 was deleted. Therefore, we assayed ^{3}H-acetate incorporation into lipids in control and CPT2KO MEFs. Consistent with the *in vivo* data, CPT2KO MEFs had a 2-fold increase in *de novo* lipogenesis from both ^{3}H-acetate and 2-^{14}C-pyruvate (Fig. 6B). Additionally, we examined the oxidation of radiolabeled 2-^{14}C-pyruvate and U-^{14}C-glucose to $^{14}CO_2$. While pyruvate oxidation was increased ~20%, glucose oxidation was increased 2-fold over control cells (Fig. 6C). These data show that the loss of fatty acid oxidation is compensated in part by increased carbohydrate flux.

Adipose fatty acid oxidation potentiates high fat diet induced oxidative stress and inflammation

The oxidation of fatty acids generates a substantial oxidative burden. It has been previously demonstrated that high fat feeding increases oxidative stress and damaging oxidative end products particularly within gWAT (Furukawa et al., 2004). Given the role of fatty acid oxidation in the generation of ROS, we profiled genes known to be involved in oxidative stress in high fat fed control and CPT2$^{A-/-}$ gWAT by qPCR array. Multiple genes involved in detoxifying ROS were increased and several more involved in generating ROS were suppressed (Fig. S4). To confirm and extend this data, we analyzed the genes and pathways identified in the qPCR screen in gWAT RNA isolated from both low and high fat fed control and CPT2$^{A-/-}$ mice. *Sod1* and *Sod2* trended towards an increase under high fat conditions and *Sod2* was significantly increased about 2-fold in low fat fed CPT2$^{A-/-}$ gWAT. Genes that increase oxidative stress were suppressed in CPT2$^{A-/-}$ gWAT specifically in high fat fed conditions (Fig. 7A). Therefore, CPT2$^{A-/-}$ gWAT gene expression was consistent with greater ROS detoxification and lower ROS generation. This led us to look at the mRNA abundance of adipokines, cytokines and inflammatory markers in gWAT of control and CPT2$^{A-/-}$ mice. *Cox2* mRNA abundance, which produces inflammatory mediators, was robustly suppressed in high fat fed CPT2$^{A-/-}$ gWAT compared to controls (Fig. 7A). *Adiponectin* mRNA abundance, which is regulated by redox and suppressed in diabetes, rebounded in high fat fed CPT2$^{A-/-}$ gWAT back to low fat fed levels (Fig. 7B). Although *Leptin* mRNA abundance in gWAT was unchanged between genotypes, *Fgf-21* and *Adipsin* were significantly suppressed in low fat fed CPT2$^{A-/-}$ mice (Fig. 7B). Since *Adipsin*, also known as complement factor D, is involved in the inflammatory response, we next looked at inflammatory markers in CPT2$^{A-/-}$ gWAT. Although, the macrophage marker *F4/80* was unchanged between CPT2$^{A-/-}$ and control mice, there was a suppression in *Cd11b* (*Mac-1*), a marker for activated macrophages, in high fat fed CPT2$^{A-/-}$ gWAT (Fig. 7C). Consistent with these changes, there was a marked suppression in inflammatory gene expression as evidenced by lower mRNA abundance of *Mip-1a* and *Il-1b*, as well as a trend for the suppression in *Mip1b* in high fat fed CPT2$^{A-/-}$ gWAT (Fig. 7C). Additionally, the mRNA abundance of the anti-inflammatory cytokine *Il-10* was significantly suppressed in high fat fed CPT2$^{A-/-}$ gWAT. There were no changes in the mRNA abundance of several important inflammatory and insulin resistance promoting cytokines/chemokines *Tnf-α*, *Il-6*, or *Mcp1* in control and CPT2$^{A-/-}$ gWAT (Fig. 7C). Finally, we measured oxidized lipids in gWAT and serum of low and high fat fed control and CPT2$^{A-/-}$ mice. The high fat diet-induced increase in lipid peroxidation observed in control gWAT and serum was repressed in CPT2$^{A-/-}$ mice (Fig. 7D). These data show that high fat feeding requires mitochondrial oxidation to potentiate high fat diet induced oxidative stress and inflammation.

Improvements in CPT2$^{A-/-}$ adipose tissue oxidative stress did not lead to improved systemic glucose tolerance

Adipose oxidative stress and inflammation induced by high fat feeding has been suggested to initiate a cascade that leads to systemic insulin resistance (Glass and Olefsky, 2012; Hotamisligil, 2010). Because we have greatly suppressed oxidative stress and improved inflammatory markers in CPT2$^{A-/-}$ mice fed a high fat diet, we determined glucose

tolerance for control and CPT2$^{A-/-}$ mice fed both low and high fat diets by glucose and insulin tolerance tests. Consistent with an increase in adiposity, low fat fed CPT2$^{A-/-}$ mice exhibited greater glucose intolerance exhibited by impaired glucose disposal during the GTT and a strong trend toward impaired glucose clearance in response to insulin in the ITT (Fig. 7E). These defects in glucose tolerance are not seen in chow fed mice, suggesting that the high content of simple sugars (i.e. sucrose) promote lipid deposition and glucose intolerance in adipose in the absence of fatty acid oxidation (Fig. S5). In contrast, high fat fed control and CPT2$^{A-/-}$ mice had similar glucose dynamics (Fig. 7F). Therefore, the improvements in adiposity, oxidative stress and inflammation in high fat fed CPT2$^{A-/-}$ mice were not sufficient to reverse systemic insulin resistance and glucose intolerance, and is not consistent with a requirement for adipose derived ROS in mediating systemic glucose intolerance.

DISCUSSION

Obesity is the result of energy imbalance. As caloric intake exceeds expenditure, metabolic flux is directed into energy reserves, primarily as triglyceride in adipose tissue. Conversely, when caloric expenditure exceeds intake, these reserves are mobilized to provide physiological fuel. Alterations in adipocyte specific metabolism can lead to systemic changes in adiposity, body weight and glucose tolerance (Abel et al., 2001; Ahmadian et al., 2011; Lodhi et al., 2012; Vernochet et al., 2012). The suppression of adipocyte fatty acid oxidation is often invoked as a mechanism to explain mouse models that are obese in the absence of increased food intake. Although this is not an implausible idea, it has lacked an experimental underpinning. Contrary to this notion, we have shown that the lack of adipocyte long chain fatty acid oxidation does not lead to changes in body weight under standard laboratory conditions even when challenged by calorically dense diets.

Brown adipose tissue can dramatically increase metabolic rate and dissipate large amounts of stored lipids in a relatively short time once activated. Transgenic mice with increased BAT mass correlate nicely with resistance to weight gain (Harms and Seale, 2013). The transplantation of large amounts of BAT into mice improves their glucose tolerance but does little to improve their body weight (Stanford et al., 2013). This may point to a robust endocrine rather than bioenergetic contribution of BAT. In fact in the absence of cold induced activation, the role of brown adipocyte bioenergetics in obesity remains controversial (Kozak, 2010). Similar to CPT2$^{A-/-}$ mice, UCP1KO mice are resistant to, rather than prone to, diet induced obesity at 20°C (Liu et al., 2003). Aging or a thermoneutral environment can alter this phenotype to produce obese prone UCP1KO mice (Feldmann et al., 2009; Kontani et al., 2005). Additionally, the loss of ACSL1 in adipocytes, which renders mice unable to efficiently activate fatty acids for oxidation, have an increase in adiposity with low fat feeding similar to CPT2$^{A-/-}$ mice (Ellis et al., 2010). Activation of catabolic processes in tissue other than adipose, needed to maintain body temperature, likely accounts for their lack of body weight change and altered adiposity (Bal et al., 2012). These experiments illuminate a compensatory role of basal metabolic rate to compensate for the loss of BAT mediated thermogenesis, however little is known about how the basal metabolic rate is regulated, where it emanates from or mechanistically how it contributes to body temperature or body weight.

The phosphorylation of CREB by adrenergic stimulation induces the robust expression of thermogenic genes in BAT including *Ucp1* and *Pgc1α*. Conversely, several nuclear hormone receptors and co-repressors such as LXRα and RIP140 negatively regulate thermogenic genes (Leonardsson et al., 2004; Wang et al., 2008). LXRα selectively represses *Ucp1* induction by binding adjacent to CREB on the *Ucp1* promoter. The cross talk between fatty acid metabolism and thermogenic programing is likely mediated by fatty acid metabolites acting as ligands for nuclear hormone receptors to suppress agonist induced transcriptional control. The fact that ACSL1$^{A-/-}$ mice are cold intolerant but still retain thermogenic gene induction suggests the defect in CPT2$^{A-/-}$ BAT gene expression lies between the activation of fatty acids and their oxidation (Ellis et al., 2010). Similar to CPT2$^{A-/-}$ mice, systemic carnitine deficiency also results in a suppression of *Ucp1* expression in BAT (Ozaki et al., 2011). These data suggest that an accumulation of fatty acid metabolites, such as long chain acyl-CoAs for example, may be critical nuclear hormone ligands acting as negative metabolic feedback sensors to link metabolic capacity to nuclear encoded mitochondrial gene expression.

Although CPT2$^{A-/-}$ mice were unable to generate heat or oxidize fatty acids in BAT and WAT, they did not have changes in body weight when fed standard chow, low fat or high fat diets. Under low fat feeding, the mice gained more adiposity, but this was likely due to the high sucrose content in the diet as chow feeding did not elicit increased adiposity. Low fat fed mice have enhanced *de novo* fatty acid synthesis in WAT likely in part due to decreased concentrations of cellular L-carnitine and acetyl-carnitine. Lower L-carnitine and acetyl-carnitine levels can shift mitochondria to increased *de novo* lipogenesis by the inability to dissipate mitochondrial acetyl-CoA and thereby its allosteric effects on the Pyruvate Dehydrogenase complex and Pyruvate Carboxylase (Muoio et al., 2012). High fat feeding elicited a suppression in adiposity in CPT2$^{A-/-}$ mice and a concomitant ~2-fold increase in circulating ketones. Severe forms of cold intolerance such as ACSL1$^{A-/-}$, CPT2$^{A-/-}$ mice, and UCP1KO mice are either neutral or mildly resistant to high-fat diet induced obesity at room temperature (Ellis et al., 2010; Liu et al., 2003). However, mouse models with mild cold intolerance are obese prone at room temperature (Liu et al., 2014; Muller et al., 2013). One possible explanation for this paradox is that mild BAT dysfunction may evade the reflexive compensation required to maintain body temperature resulting in increased weight gain. Long term housing of mice at thermoneutrality may relieve this compensation and generate obese prone CPT2$^{A-/-}$ mice similar to UCP1KO mice (Feldmann et al., 2009). It is not clear, however, what the role of uncoupling and heat generation is at thermoneutrality. Is there still a need for BAT thermogenesis or is uncoupling required for something else entirely such as the generation of metabolic water (Neess et al., 2013; Nelson et al., 1973)?

It is clear that fatty acid oxidation is important in BAT, however, how does fatty acid oxidation in WAT contribute? The high oxidative stress and inflammation seen after long term high fat feeding has been attributed to fatty acid metabolism, which we confirm here (Furukawa et al., 2004). Here we have evidence that the rate setting step in fatty acid oxidation is transcriptionally up-regulated 6-fold in high fat fed gWAT (Fig. S2C). We also observed increases in oxidative stress and inflammation under a high fat diet and these changes are greatly reduced in the absence of adipose fatty acid oxidation. Systemic glucose

intolerance attributed to local adipose dysfunction was not, however, ameliorated by the loss of CPT2. We observed a suppression in gWAT inflammation in $CPT2^{A-/-}$ mice, as evidenced by a suppression in *Cd11b*, *Cox2*, *Mip1a*, and *Il1b*. The major and likely most relevant inflammatory mediators for insulin resistance such as *Tnf-α* and *Mcp1* for example were unchanged (Hotamisligil, 2010). Therefore, these important mediators of obesity-induced insulin resistance were not dependent on adipose mitochondrial long chain fatty acid beta-oxidation.

In summary, adipose tissue fatty acid oxidation is critical for acute adaptation to the cold by providing both the energy required to fuel heat generation and the transcriptional regulation of BAT thermogenesis. Additionally, white adipose fatty acid oxidation potentiates high fat diet induced oxidative stress and inflammation, however, the improvements seen in $CPT2^{A-/-}$ mice were not sufficient to reverse systemic insulin resistance. Taken together, adipose fatty acid oxidation is an important metabolic process for environmental and nutritional homeostasis.

EXPERIMENTAL PROCEDURES

Animals and diets

$CPT2^{lox/lox}$ mice were generated by targeting loxP sequences to introns flanking exon 4 of the mouse *Cpt2* gene by homologous recombination in C57Bl/6 embryonic stem cells by standard methods. To produce mice with a loss of CPT2 specifically in adipocytes, we bred $CPT2^{lox/lox}$ mice to Adiponectin-Cre transgenic mice (Eguchi et al., 2011). $CPT2^{A-/-}$ and littermate $CPT2^{lox/lox}$ mice were housed in a facility with ventilated racks on a 14 h light/10 h dark cycle with access to a standard chow diet (Etruded Global Rodent Diet, Harlan Laboratories). For the diet study, mice were fed a 10% low fat (D12450J, Research Diets) or a 60% high fat diet (D12492, Research Diets) from 6 weeks to 18 weeks of age (12 weeks on diet). At week 10 of the diet, mice were subjected to a glucose tolerance test by intraperitoneal injection of glucose (0.75g/kg) and measuring tail blood glucose at 0, 15, 30, 60 and 120 minutes. At week 11 of the diet, insulin tolerance tests were performed via intraperitoneal injection of insulin (0.6 units/kg) and measuring tail blood glucose at 0, 15, 30, 60 and 90 minutes (Nova Max Plus). Body weights were measured on a weekly basis. For thermogenesis experiments, 12-week old mice had food withdrawn for 4 hours and placed in a 4°C environment for 3 hours. Body temperature was measured hourly by a rectal probe thermometer (BAT-12, Physitemp). BAT, iWAT, gWAT, liver, and muscle were collected and frozen in liquid nitrogen. Serum was collected from all mice and free glycerol and TAG (Sigma), β-hydroxybutyrate (StanBio), total cholesterol (Wako) and NEFA (Wako) were measured colorimetrically. BAT collected from thermogenesis experiments was homogenized in Media I (10mM Tris pH 8.0, 1mM EDTA and 0.25M Sucrose) to measure TAG (Sigma). For *in vivo* studies, 20-week old $CPT2^{A-/-}$ and littermate $CPT2^{lox/lox}$ mice were injected with CL-316243 (10mg/kg, Santa Cruz) or vehicle. To determine the protein expression of phospho-CREB, CREB, phospho-mTOR and mTOR, CL-316243 (10mg/kg) or vehicle was injected to 20-week old mice and tissues were collected after 30min. For cold acclimation, 12–14 week old $CPT2^{A-/-}$ and littermate $CPT2^{lox/lox}$ mice were housed in an animal incubator at 18°C on a 12h light/12 h dark cycle

with access to a standard chow diet for one week. The incubator was lowered to 15°C the following week. Then mice had food withdrawn for 4 hours and placed in a 4°C environment for 4 hours. For thermoneutral adaptation, 12-week old $CPT2^{A-/-}$ and littermate $CPT2^{lox/lox}$ mice were housed in an animal incubator at 30°C on a 12h light/12 h dark cycle with access to a standard chow diet for 2 weeks. At 14 weeks of age, the mice were injected with either CL-316243 (10mg/kg) or vehicle for 3 hours. All procedures were performed in accordance with the National Institutes of Health Guide for the Care and Use of Laboratory Animals and under the approval of the Johns Hopkins Medical School Animal Care and Use Committee.

Body composition and metabolic analysis

Body fat and lean mass were determined by magnetic resonance imaging (minispec MQ10) in 18-week old mice. To measure whole animal energy utilization, 12-week old male $CPT2^{A-/-}$ and $CPT2^{lox/lox}$ littermates that were fed a standard chow diet were individually housed in Comprehensive Laboratory Animal Monitoring System (CLAMS, Columbus instruments) cages on a 12 h light/12 h dark cycle. O_2 and CO_2 consumption and production respectively, food and water intake, and home cage activity were measured continuously. After a 2-day acclimation period, data were collected for 48 hours for *ad libitum*, and a 24-hour fasting period. At the end of the study, the same mice were injected with CL-316243 (10mg/kg) and were monitored for 3 hours.

In vivo acetate incorporation experiment

6-week old $CPT2^{A-/-}$ and littermate $CPT2^{lox/lox}$ mice were fed a 10% low fat diet for 2 weeks. At 8 weeks of age, mice were injected with 10μCi of [^{3}H] acetate for 3 hours. BAT, gWAT, and liver were collected and lipid was extracted using the Folch method. Aliquots of the samples were counted for [^{3}H] labeled lipids. All samples were counted using the Beckman Coulter scintillation counter (LS 6000SC, Beckman Coulter).

Cell culture

$CPT2^{lox/lox}$ primary mouse embryonic fibroblasts (MEFs) were derived from embryos and cultured in Dulbecco's Modified Eagle Medium (DMEM) supplemented with 10% fetal bovine serum (FBS) and 1% penicillin/streptomycin. To generate $CPT2^{lox/lox}$ and CPT2KO MEFs, cells were first transduced with large T antigen-expressing lentiviral particles (LVP016-Neo, GenTarget Inc) for 48 hours and G418 (300μg/mL) was added to select for positive cells. The selected cells were then transduced with RFP (LVP023, GenTarget Inc) or CRE-2A-RFP (LVP013, GenTarget Inc) lentiviral particles and selected with blasticidin (10μg/mL) to generate $CPT2^{lox/lox}$ and CPT2KO MEFs, respectively.

MEFs were plated in T25 flasks at 70% confluency and incubated in DMEM supplemented with 10% FBS and 1% penicillin/streptomycin overnight. The cells were washed with 1X PBS and the reaction mixture for [U-^{14}C] glucose (DMEM (A14430-01), 2mM glutamine, 2.5mM glucose, 0.5mM sodium pyruvate, 0.1μCi of [U-^{14}C] glucose) or [2-^{14}C] pyruvate (DMEM (A14430-01), 2mM glutamine, 2.5mM glucose, 0.5mM sodium pyruvate, 0.1μCi of [2-^{14}C] pyruvate) was added to cells. The flasks were sealed with a rubber stopper containing a hanging well filled with filter paper and incubated in a 37°C incubator for 4

hours. Carbon dioxide was trapped by adding 150μL of 1M NaOH to the filter paper in the center well and 200μL of 1M perchloric acid to the reaction mixture. Then the samples were incubated at 55°C for one hour and the filter paper was placed in scintillation fluid and counted. For [1-^{14}C] oleate oxidation, the reaction mixture (DMEM supplemented with 0.1μCi of [1-^{14}C] oleate, 100μM L-Carnitine Hydrochloride (Sigma) and 0.2% BSA) or the reaction mixture containing 100μM etomoxir was added to cells and incubated in a 37°C incubator for 4 hours. Carbon dioxide was collected and counted as described above. For [1-^{14}C] lignoceric acid oxidation, the reaction mixture (DMEM supplemented with 0.1μCi of [1-^{14}C] lignocerate and 0.2% BSA) was added to cells and incubated overnight in a 37°C incubator. Carbon dioxide was collected and counted as described above.

For substrate flux into lipids, MEFs were plated in 24-well plates and incubated in DMEM supplemented with 10% FBS and 1% penicillin/streptomycin overnight and washed with 1X PBS the next day. The cells were incubated in [2-^{14}C] pyruvate (DMEM (A14430-01), 2mM glutamine, 2.5mM glucose, 0.5mM sodium pyruvate, 0.1μCi of [2-^{14}C] pyruvate) or [^{3}H] acetate (DMEM supplemented with 0.3μCi [^{3}H] acetate) reaction mixture and incubated at 37°C for 4 hours. Lipid was extracted using the Folch method and aliquots of the samples were counted for [^{3}H] labeled lipids.

Adipose tissue oxidation experiments

BAT, iWAT, and gWAT were collected from 20-week old CPT2$^{A-/-}$ and littermate CPT2$^{lox/lox}$ male mice and placed in an incubation chamber containing the reaction mixture (DMEM supplemented with 0.1uCi of [1-^{14}C] oleate, 100μM L-Carnitine (Sigma) and 0.2% BSA). The chamber contained a center well filled with filter paper and sealed with a rubber stopper. The incubation chambers were in a 37°C shaking water bath for 4 hours. Trapping carbon dioxide was collected as described above. In vivo fatty acid oxidation was carried out as previously described (Reamy and Wolfgang, 2011; Rodriguez and Wolfgang, 2012).

BAT explant experiments

BAT was collected from 20-week old mice. Each BAT nugget was cut in half and placed in media (DMEM, 10% FBS, 200μM total of Palmitate and Oleate at a 1:2 molar ratio, BSA at a 1:3 molar ratio with total fatty acids). Forskolin (10uM, Sigma), Isoproterenol (10uM, Sigma) or CL-316243 (10uM, Santa Cruz) was added to tubes and incubated in a 37°C water bath for 3 hours. The tissues were frozen in liquid nitrogen for further analysis.

Analysis of Gene Expression and Mitochondrial DNA (mtDNA) by Quantitative PCR

Total RNA was isolated using the RNeasy Mini Kit (Qiagen). 1–2 μg of RNA was reverse transcribed using the High Capacity cDNA Reverse Transcription Kit (Applied Biosciences). The cDNA was diluted to 2ng/μL and was amplified by specific primers in a 20μL reaction using SsoAdvanced SYBR Green Supermix (Biorad). WAT cDNA from CPT2$^{A-/-}$ and littermate CPT2$^{lox/lox}$ mice on HFD was prepared according to the manufacturer's protocol for the mouse oxidative stress PCR array (SABiosciences). Analysis of gene expression was carried out in a CFX Connect Real-Time System (Biorad). For each gene, mRNA expression was calculated as 2^deltaCT relative to Cyclophilin A expression. For mtDNA analysis, total DNA was prepared using the QIAmp DNA mini Kit

(Qiagen). Mitochondrial DNA was amplified using primers Co1 and Nd1 and was normalized to genomic DNA by primers amplifying H19 from genomic DNA as previously described (Ellis et al., 2011). Primers and gene information are provided in Table S1.

Western blot analysis

BAT collected after acute CL-316243 or vehicle injection was homogenized in 1X RIPA buffer with protease inhibitors (Complete Mini, Roche) and phosphatase inhibitors (PhosSTOP, Roche). All other tissues from the diet study were homogenized in 1X RIPA buffer with protease inhibitors (Complete Mini, Roche). BAT, gWAT, iWAT and liver samples from thermogenesis experiments were homogenized in Media I with protease inhibitors. All samples were spun down at 10,000RPM for 20 minutes and supernatant was collected and assayed by the Pierce BCA Protein Assay Kit (Thermo Scientific) to determine the concentration of protein. 30μg of protein were subjected to SDS-PAGE and transferred to a nitrocellulose membrane (Protran BA 83, Whatman). The blots were probed with the following antibodies:

Uqcrc2 (mitoprofile Total OXPHOS, Abcam), Sdhb (mitoprofile Total OXPHOS, Abcam), Acsf3 (Pierce), phospho-CREB (Ser-133, Millipore), CREB (Pierce), phospho-mTOR (Cell Signaling), and mTOR (Cell Signaling) used the appropriate secondary antibodies conjugated to horseradish peroxidase (HRP). Fasn (BD Biosciences), Aco2 (Cell Signaling), Mcad (GeneTex), Hsc70 (Santa Cruz), Sod2, Hadha (GeneTex) used the appropriate Cy5 (Life Techonologies) or Cy3 (Life Techonologies) fluorescent secondary antibodies.

Oxidative damage

Thiobarbituric acid reactive substances (TBARS) were determined in gWAT, and serum from 20-week old male $CPT2^{A-/-}$ and littermate $CPT2^{lox/lox}$ mice fed HFD or LFD. WAT was prepared by homogenizing 100mg of tissue in 500μL of 1X RIPA buffer with protease inhibitors (Complete Mini, Roche). Homogenates were centrifuged at 1,600 × g for 10 minutes and 25μL of supernatant was used to determine oxidative damage via the TBARS Assay Kit (Cayman Chemical Company).

Acylcarnitine analysis

iWAT from $CPT2^{A-/-}$ and littermate $CPT2^{lox/lox}$ mice were collected and frozen in liquid nitrogen. ~100mg of tissue were analyzed for acylcarnitine content at the University of Michigan Metabolomics Core Services.

Statistical analysis

When only two genotypes were analyzed, statistical significance was determined using a student's t-test. Two-way ANOVA was utilized for repeated measures such as body temperature over time, weight gain over time, GTT and ITT. Significance was determined for values $p<0.05$.

Supplementary Material

Refer to Web version on PubMed Central for supplementary material.

Acknowledgments

The authors would like to thank Susan Aja for assistance with the metabolic cage studies, Natasha Zachara for reagents and G. W. Wong for helpful discussions. This work was supported in part by a National Institutes of Health grant R01NS072241 to M.J.W. This work utilized Metabolomics Core Services supported by grant U24 DK097153 of NIH Common Funds Project to the University of Michigan.

References

Abel ED, Peroni O, Kim JK, Kim YB, Boss O, Hadro E, Minnemann T, Shulman GI, Kahn BB. Adipose-selective targeting of the GLUT4 gene impairs insulin action in muscle and liver. Nature. 2001; 409:729–733. [PubMed: 11217863]

Abu-Elheiga L, Matzuk MM, Abo-Hashema KA, Wakil SJ. Continuous fatty acid oxidation and reduced fat storage in mice lacking acetyl-CoA carboxylase 2. Science. 2001; 291:2613–2616. [PubMed: 11283375]

Ahmadian M, Abbott MJ, Tang T, Hudak CS, Kim Y, Bruss M, Hellerstein MK, Lee HY, Samuel VT, Shulman GI, et al. Desnutrin/ATGL is regulated by AMPK and is required for a brown adipose phenotype. Cell metabolism. 2011; 13:739–748. [PubMed: 21641555]

Bal NC, Maurya SK, Sopariwala DH, Sahoo SK, Gupta SC, Shaikh SA, Pant M, Rowland LA, Bombardier E, Goonasekera SA, et al. Sarcolipin is a newly identified regulator of muscle-based thermogenesis in mammals. Nature medicine. 2012; 18:1575–1579.

Eguchi J, Wang X, Yu S, Kershaw EE, Chiu PC, Dushay J, Estall JL, Klein U, Maratos-Flier E, Rosen ED. Transcriptional control of adipose lipid handling by IRF4. Cell metabolism. 2011; 13:249–259. [PubMed: 21356515]

Ellis JM, Li LO, Wu PC, Koves TR, Ilkayeva O, Stevens RD, Watkins SM, Muoio DM, Coleman RA. Adipose acyl-CoA synthetase-1 directs fatty acids toward beta-oxidation and is required for cold thermogenesis. Cell metabolism. 2010; 12:53–64. [PubMed: 20620995]

Ellis JM, Mentock SM, Depetrillo MA, Koves TR, Sen S, Watkins SM, Muoio DM, Cline GW, Taegtmeyer H, Shulman GI, et al. Mouse cardiac acyl coenzyme a synthetase 1 deficiency impairs Fatty Acid oxidation and induces cardiac hypertrophy. Molecular and cellular biology. 2011; 31:1252–1262. [PubMed: 21245374]

Feldmann HM, Golozoubova V, Cannon B, Nedergaard J. UCP1 ablation induces obesity and abolishes diet-induced thermogenesis in mice exempt from thermal stress by living at thermoneutrality. Cell metabolism. 2009; 9:203–209. [PubMed: 19187776]

Furukawa S, Fujita T, Shimabukuro M, Iwaki M, Yamada Y, Nakajima Y, Nakayama O, Makishima M, Matsuda M, Shimomura I. Increased oxidative stress in obesity and its impact on metabolic syndrome. The Journal of clinical investigation. 2004; 114:1752–1761. [PubMed: 15599400]

Glass CK, Olefsky JM. Inflammation and lipid signaling in the etiology of insulin resistance. Cell metabolism. 2012; 15:635–645. [PubMed: 22560216]

Golozoubova V, Hohtola E, Matthias A, Jacobsson A, Cannon B, Nedergaard J. Only UCP1 can mediate adaptive nonshivering thermogenesis in the cold. FASEB journal: official publication of the Federation of American Societies for Experimental Biology. 2001; 15:2048–2050. [PubMed: 11511509]

Guerra C, Koza RA, Walsh K, Kurtz DM, Wood PA, Kozak LP. Abnormal nonshivering thermogenesis in mice with inherited defects of fatty acid oxidation. The Journal of clinical investigation. 1998; 102:1724–1731. [PubMed: 9802886]

Harms M, Seale P. Brown and beige fat: development, function and therapeutic potential. Nature medicine. 2013; 19:1252–1263.

Haynie KR, Vandanmagsar B, Wicks SE, Zhang J, Mynatt RL. Inhibition of carnitine palymitoyltransferase1b induces cardiac hypertrophy and mortality in mice. Diabetes Obes Metab. 2014; 16:757–760. [PubMed: 24330405]

Hotamisligil GS. Endoplasmic reticulum stress and the inflammatory basis of metabolic disease. Cell. 2010; 140:900–917. [PubMed: 20303879]

Houstis N, Rosen ED, Lander ES. Reactive oxygen species have a causal role in multiple forms of insulin resistance. Nature. 2006; 440:944–948. [PubMed: 16612386]

Hsiao YS, Jogl G, Esser V, Tong L. Crystal structure of rat carnitine palmitoyltransferase II (CPT-II). Biochemical and biophysical research communications. 2006; 346:974–980. [PubMed: 16781677]

Ji S, You Y, Kerner J, Hoppel CL, Schoeb TR, Chick WS, Hamm DA, Sharer JD, Wood PA. Homozygous carnitine palmitoyltransferase 1b (muscle isoform) deficiency is lethal in the mouse. Molecular genetics and metabolism. 2008; 93:314–322. [PubMed: 18023382]

Keaney JF Jr, Larson MG, Vasan RS, Wilson PW, Lipinska I, Corey D, Massaro JM, Sutherland P, Vita JA, Benjamin EJ. Obesity and systemic oxidative stress: clinical correlates of oxidative stress in the Framingham Study. Arterioscler Thromb Vasc Biol. 2003; 23:434–439. [PubMed: 12615693]

Kontani Y, Wang Y, Kimura K, Inokuma KI, Saito M, Suzuki-Miura T, Wang Z, Sato Y, Mori N, Yamashita H. UCP1 deficiency increases susceptibility to diet-induced obesity with age. Aging Cell. 2005; 4:147–155. [PubMed: 15924571]

Kozak LP. Brown fat and the myth of diet-induced thermogenesis. Cell metabolism. 2010; 11:263–267. [PubMed: 20374958]

Kusminski CM, Scherer PE. Mitochondrial dysfunction in white adipose tissue. Trends Endocrinol Metab. 2012; 23:435–443. [PubMed: 22784416]

Leonardsson G, Steel JH, Christian M, Pocock V, Milligan S, Bell J, So PW, Medina-Gomez G, Vidal-Puig A, White R, et al. Nuclear receptor corepressor RIP140 regulates fat accumulation. Proceedings of the National Academy of Sciences of the United States of America. 2004; 101:8437–8442. [PubMed: 15155905]

Liu M, Bai J, He S, Villarreal R, Hu D, Zhang C, Yang X, Liang H, Slaga TJ, Yu Y, et al. Grb10 Promotes Lipolysis and Thermogenesis by Phosphorylation-Dependent Feedback Inhibition of mTORC1. Cell metabolism. 2014; 19:967–980. [PubMed: 24746805]

Liu X, Rossmeisl M, McClaine J, Riachi M, Harper ME, Kozak LP. Paradoxical resistance to diet-induced obesity in UCP1-deficient mice. The Journal of clinical investigation. 2003; 111:399–407. [PubMed: 12569166]

Lodhi IJ, Yin L, Jensen-Urstad AP, Funai K, Coleman T, Baird JH, El Ramahi MK, Razani B, Song H, Fu-Hsu F, et al. Inhibiting adipose tissue lipogenesis reprograms thermogenesis and PPARgamma activation to decrease diet-induced obesity. Cell metabolism. 2012; 16:189–201. [PubMed: 22863804]

Longo N, Amat di San Filippo C, Pasquali M. Disorders of carnitine transport and the carnitine cycle. Am J Med Genet C Semin Med Genet. 2006; 142C:77–85. [PubMed: 16602102]

Lowell BB, VSS, Hamann A, Lawitts JA, Himms-Hagen J, Boyer BB, Kozak LP, Flier JS. Development of obesity in transgenic mice after genetic ablation of brown adipose tissue. Nature. 1993; 366:740–742. [PubMed: 8264795]

Muller TD, Lee SJ, Jastroch M, Kabra D, Stemmer K, Aichler M, Abplanalp B, Ananthakrishnan G, Bhardwaj N, Collins S, et al. p62 links beta-adrenergic input to mitochondrial function and thermogenesis. The Journal of clinical investigation. 2013; 123:469–478. [PubMed: 23257354]

Muoio DM, Noland RC, Kovalik JP, Seiler SE, Davies MN, DeBalsi KL, Ilkayeva OR, Stevens RD, Kheterpal I, Zhang J, et al. Muscle-specific deletion of carnitine acetyltransferase compromises glucose tolerance and metabolic flexibility. Cell metabolism. 2012; 15:764–777. [PubMed: 22560225]

Neess D, Bek S, Bloksgaard M, Marcher AB, Faergeman NJ, Mandrup S. Delayed hepatic adaptation to weaning in ACBP−/− mice is caused by disruption of the epidermal barrier. Cell Rep. 2013; 5:1403–1412. [PubMed: 24316079]

Nelson RA, Wahner HW, Jones JD, Ellefson RD, Zollman PE. Metabolism of bears before, during, and after winter sleep. The American journal of physiology. 1973; 224:491–496. [PubMed: 4686505]

Nyman LR, Cox KB, Hoppel CL, Kerner J, Barnoski BL, Hamm DA, Tian L, Schoeb TR, Wood PA. Homozygous carnitine palmitoyltransferase 1a (liver isoform) deficiency is lethal in the mouse. Mol Genet Metab. 2005; 86:179–187. [PubMed: 16169268]

Ozaki K, Sano T, Tsuji N, Matsuura T, Narama I. Carnitine is necessary to maintain the phenotype and function of brown adipose tissue. Lab Invest. 2011; 91:704–710. [PubMed: 21321536]

Reamy AA, Wolfgang MJ. Carnitine palmitoyltransferase-1c gain-of-function in the brain results in postnatal microencephaly. Journal of neurochemistry. 2011; 118:388–398. [PubMed: 21592121]

Rodriguez S, Wolfgang MJ. Targeted chemical-genetic regulation of protein stability in vivo. Chemistry & biology. 2012; 19:391–398. [PubMed: 22444594]

Schuler AM, Gower BA, Matern D, Rinaldo P, Vockley J, Wood PA. Synergistic heterozygosity in mice with inherited enzyme deficiencies of mitochondrial fatty acid beta-oxidation. Molecular genetics and metabolism. 2005; 85:7–11. [PubMed: 15862275]

Stanford KI, Middelbeek RJ, Townsend KL, An D, Nygaard EB, Hitchcox KM, Markan KR, Nakano K, Hirshman MF, Tseng YH, et al. Brown adipose tissue regulates glucose homeostasis and insulin sensitivity. The Journal of clinical investigation. 2013; 123:215–223. [PubMed: 23221344]

Tolwani RJ, Hamm DA, Tian L, Sharer JD, Vockley J, Rinaldo P, Matern D, Schoeb TR, Wood PA. Medium-chain acyl-CoA dehydrogenase deficiency in gene-targeted mice. PLoS genetics. 2005; 1:e23. [PubMed: 16121256]

Tseng YH, Cypess AM, Kahn CR. Cellular bioenergetics as a target for obesity therapy. Nat Rev Drug Discov. 2010; 9:465–482. [PubMed: 20514071]

Ukropec J, Anunciado RP, Ravussin Y, Hulver MW, Kozak LP. UCP1-independent thermogenesis in white adipose tissue of cold-acclimated Ucp1−/− mice. The Journal of biological chemistry. 2006; 281:31894–31908. [PubMed: 16914547]

Vernochet C, Mourier A, Bezy O, Macotela Y, Boucher J, Rardin MJ, An D, Lee KY, Ilkayeva OR, Zingaretti CM, et al. Adipose-specific deletion of TFAM increases mitochondrial oxidation and protects mice against obesity and insulin resistance. Cell metabolism. 2012; 16:765–776. [PubMed: 23168219]

Wang H, Zhang Y, Yehuda-Shnaidman E, Medvedev AV, Kumar N, Daniel KW, Robidoux J, Czech MP, Mangelsdorf DJ, Collins S. Liver X receptor alpha is a transcriptional repressor of the uncoupling protein 1 gene and the brown fat phenotype. Molecular and cellular biology. 2008; 28:2187–2200. [PubMed: 18195045]

Wang T, Zang Y, Ling W, Corkey BE, Guo W. Metabolic partitioning of endogenous fatty acid in adipocytes. Obes Res. 2003; 11:880–887. [PubMed: 12855758]

Wolfgang MJ, Lane MD. Control of energy homeostasis: role of enzymes and intermediates of fatty acid metabolism in the central nervous system. Annu Rev Nutr. 2006; 26:23–44. [PubMed: 16704352]

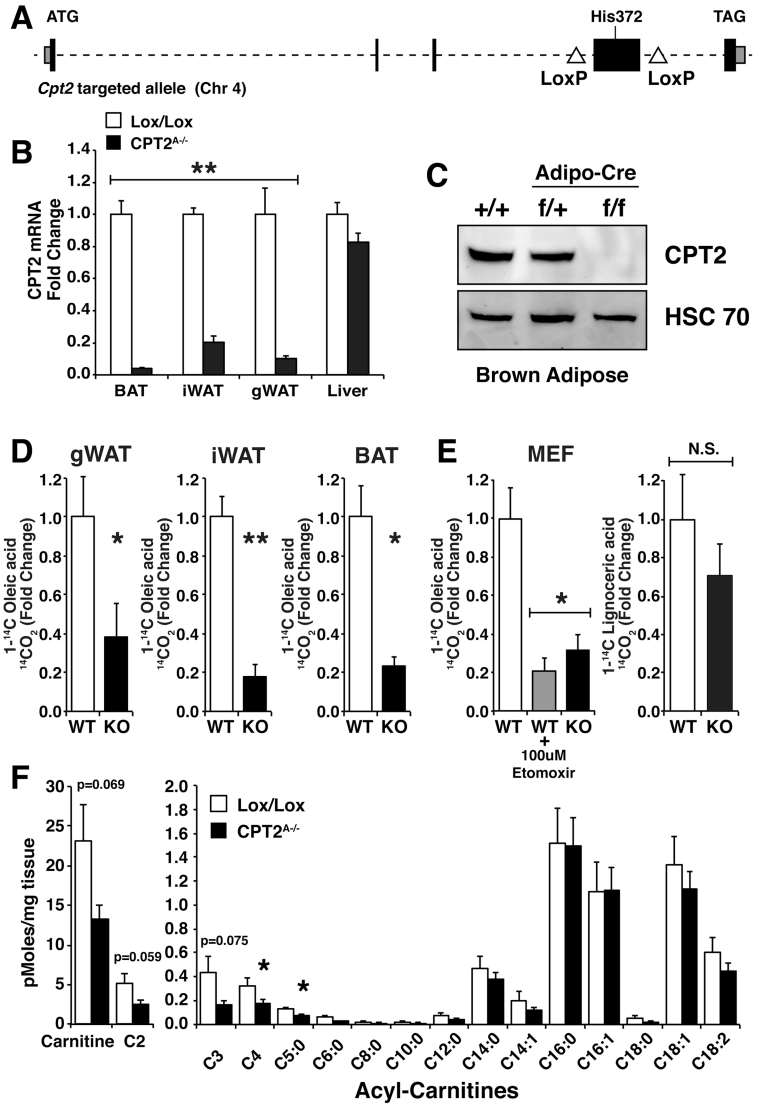

Figure 1. Generation of mice with an adipose specific KO of CPT2

(A) Gene targeting strategy for the *Cpt2* gene. Triangles represent LoxP sites.

(B) mRNA for *Cpt2* in adipose depots and liver of control and CPT2$^{A-/-}$ mice (n=8).

(C) Western blot for CPT2 in BAT of control, CPT2$^{A-/+}$ and CPT2$^{A-/-}$ mice.

(D) Oxidation of 1-^{14}C-Oleic acid to $^{14}CO_2$ in control and CPT2$^{A-/-}$ adipose depot explants (n=5).

(E) Oxidation of 1-^{14}C-Oleic acid or 1-^{14}C-Lignoceric acid to $^{14}CO_2$ in control and CPT2 KO MEFs (n=5).

(F) Acyl-Carnitine profile of iWAT in control and CPT2$^{A-/-}$ mice (n=8). Data are expressed as means +/− SEM. *p<0.05, **p<0.001, N.S. not significant. Open bars represent control and black bars represent loss of CPT2.

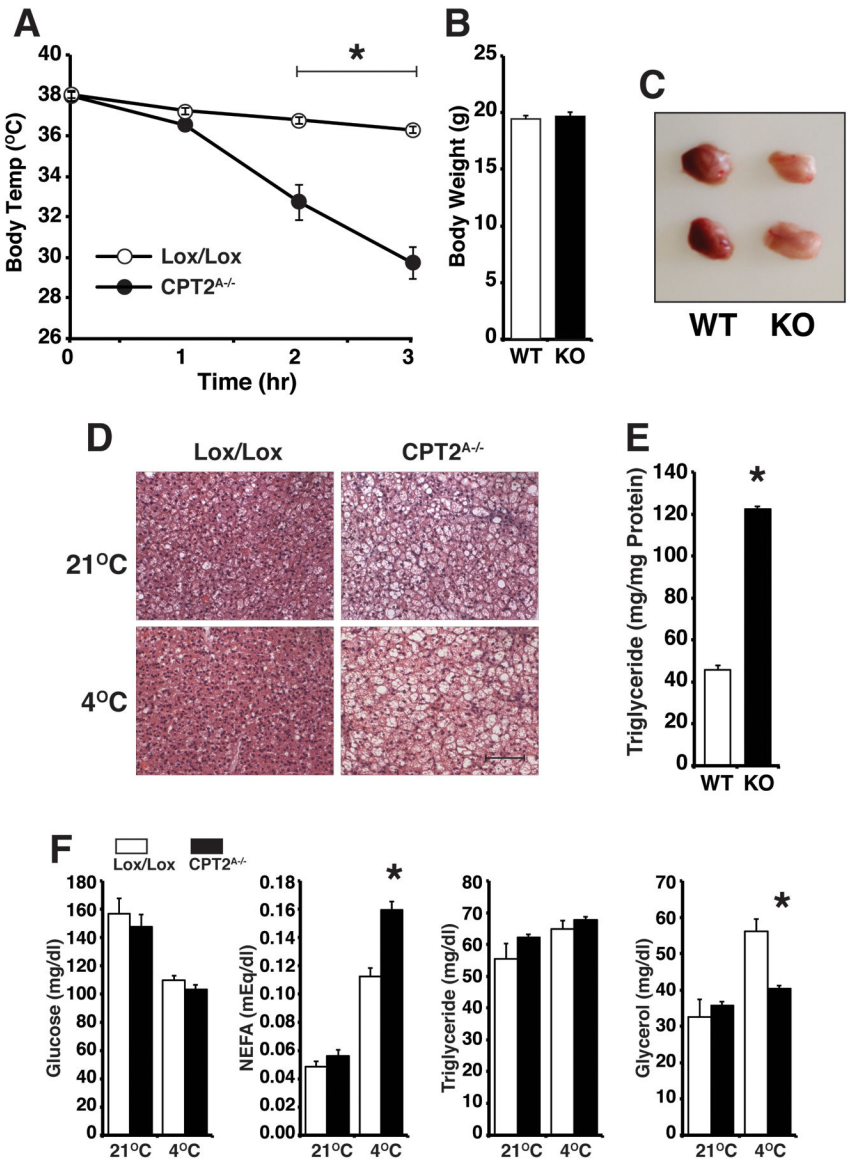

Figure 2. Adipose fatty acid oxidation is required for acute cold induced thermogenesis

(A) Body temperature of control and CPT2$^{A-/-}$ mice subjected to a 3hr cold challenge (n=10–13).

(B) Body weights of 12 week old female control and CPT2$^{A-/-}$ mice (n=22–26).

(C) Gross morphology of control and CPT2$^{A-/-}$ BAT after 2hr of cold exposure.

(D) H&E stained sections of BAT from control and CPT2$^{A-/-}$ mice at 21°C and 3hr at 4°C. Scale bar is 100μM.

(E) Triglyceride content of BAT of control and CPT2$^{A-/-}$ mice after 3hr at 4°C (n=5).

(F) Serum metabolites in control and CPT2$^{A-/-}$ mice at 21°C and 3hr at 4°C (n=8). Data are expressed as means +/− SEM. *p<0.001. Open bars represent control and black bars represent loss of CPT2.

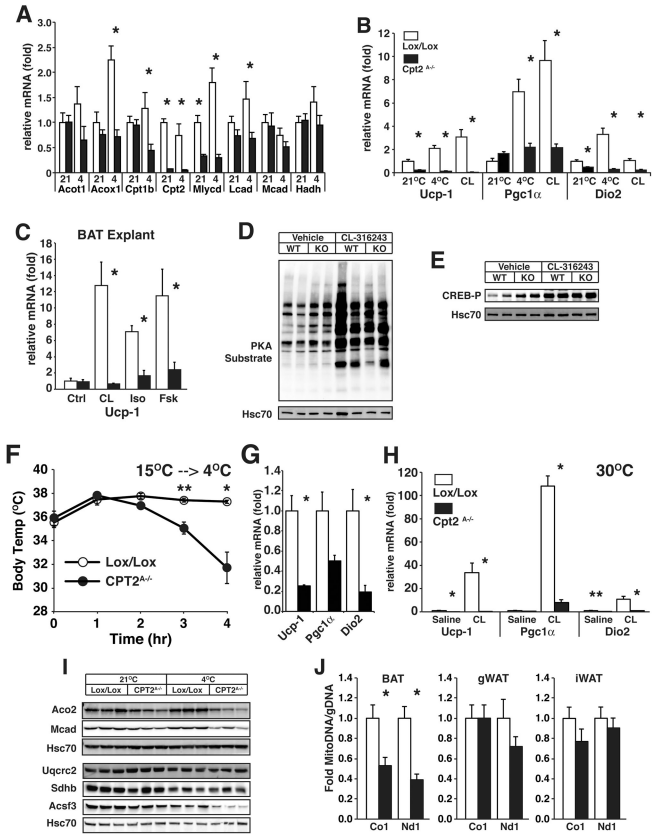

Figure 3. Adipose fatty acid oxidation is required for agonist induced thermogenic gene expression and mitochondrial homeostasis

(A) mRNA expression of fatty acid oxidative genes in BAT of control and CPT2$^{A-/-}$ mice at 21°C or after 3hr at 4°C (n=8).

(B) mRNA expression of *Ucp1*, *Pgc1α*, and *Dio2* in BAT of control and CPT2$^{A-/-}$ mice at 21°C (n=8), after 3hr at 4°C (n=8), or 3hr after injection with 10mg/kg CL-316243 (n=5).

(C) mRNA expression of *Ucp1* in BAT explants treated with 10uM CL-316243, isoproterenol, or forskolin (n=5).

(D) Western blot for PKA phosphorylated substrates in BAT of control and CPT2$^{A-/-}$ mice treated with 10mg/kg CL-316243 for 30min *in vivo*.

(E) Western blot for P-CREB (Ser-133) in BAT of control and CPT2$^{A-/-}$ mice treated with 10mg/kg CL-316243 for 30min *in vivo*.

(F) Body temperature of control and CPT2$^{A-/-}$ mice acclimatized to 15°C and subjected to a 4hr cold challenge at 4°C (n=5).

(G) mRNA expression of *Ucp1*, *Pgc1α*, and *Dio2* in BAT of 15°C acclimatized control and CPT2$^{A-/-}$ mice after a 4hr cold challenge (n=5).

(H) mRNA expression of *Ucp1*, *Pgc1α*, and *Dio2* in BAT of control and CPT2$^{A-/-}$ mice acclimatized to 30°C and injected with vehicle or 10mg/kg CL-316243 for 3hrs (n=4–5).

(I) Western blot of mitochondrial proteins in BAT of control and CPT2$^{A-/-}$ mice at 21°C or after 3hr at 4°C.

(J) Mitochondrial DNA content of BAT and gWAT from control and CPT2$^{A-/-}$ mice (n=10–12). Data are expressed as means +/− SEM. * $p<0.01$, **$p<0.05$. Open bars represent control and black bars represent loss of CPT2.

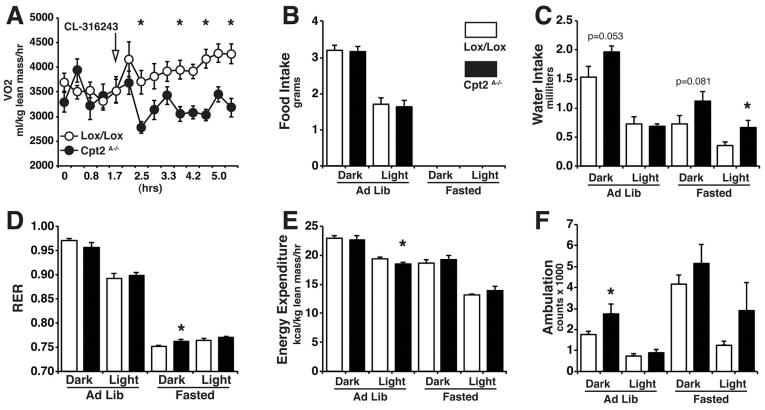

Figure 4. Contribution of adipose fatty acid oxidation to energy expenditure

(A) VO2 consumption of control and CPT2$^{A-/-}$ male mice treated with 10mg/kg CL-316243.

(B) Food intake of control and CPT2$^{A-/-}$ mice.

(C) Water intake of control and CPT2$^{A-/-}$ mice under *ad libitum* and fasting in under dark and light cycles.

(D) Respiratory Exchange Ratio of control and CPT2$^{A-/-}$ mice under *ad libitum* and fasting in under dark and light cycles.

(E) Energy expenditure of control and CPT2$^{A-/-}$ mice under *ad libitum* and fasting in under dark and light cycles.

(F) Ambulation rates of control and CPT2$^{A-/-}$ mice under *ad libitum* and fasting in under dark and light cycles (n=10–14). Data are expressed as means +/− SEM. *p<0.05. Open bars represent control and black bars represent loss of CPT2.

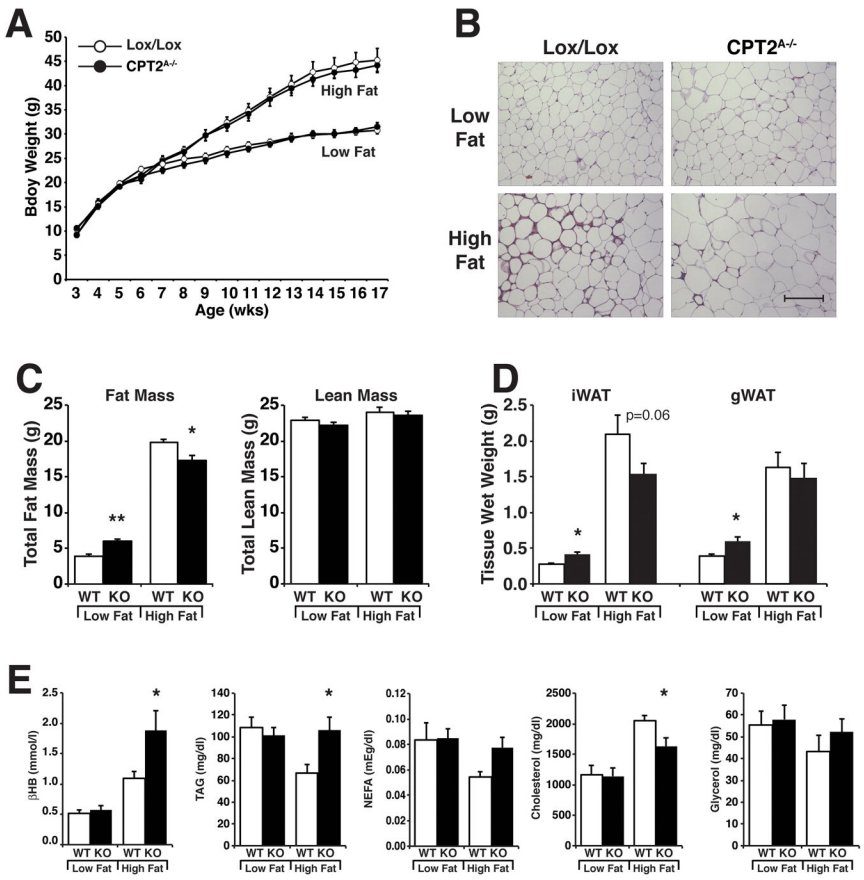

Figure 5. The loss of adipose fatty acid oxidation affects diet dependent adiposity but not body weight

(A) Body weights of control and CPT2$^{A-/-}$ male mice fed a low or high fat diet (n=13–18).

(B) H&E stained sections of gWAT from control and CPT2$^{A-/-}$ mice fed low or high fat diets. Scale bar is 250μM.

(C) Body compositions measured by EchoMRI for control and CPT2$^{A-/-}$ mice fed low or high fat diets (n=13–18).

(D) Wet weights of iWAT and gWAT unilateral depots for control and CPT2$^{A-/-}$ mice fed low or high fat diets (n=13–18).

(E) Serum metabolites in control and CPT2$^{A-/-}$ mice fed low or high fat diets (n=8). Data are expressed as means +/− SEM. **p<0.01, *p<0.05. Open bars represent control and black bars represent loss of CPT2.

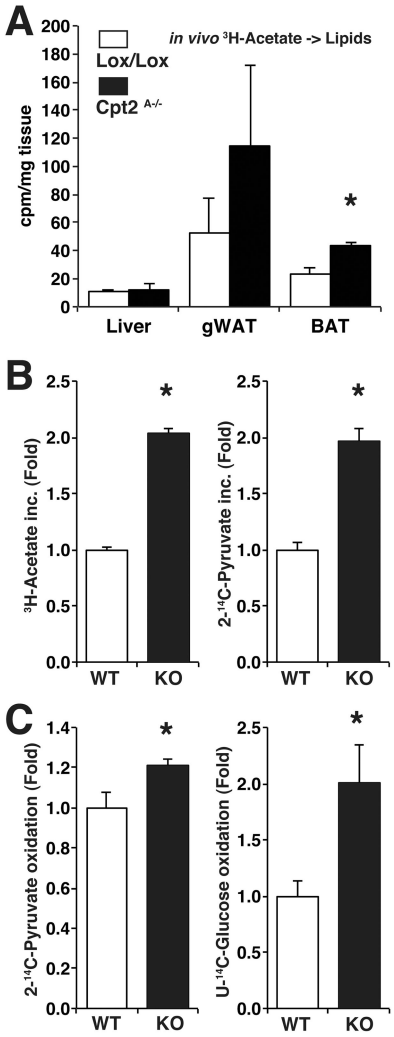

Figure 6. The loss of fatty acid oxidation alters carbohydrate metabolic flux

(A) *De novo* lipogenesis of control and CPT2$^{A-/-}$ liver, gWAT and BAT from a 1hr injection of ^{3}H-Acetate normalized to tissue wet weight. (n=4–5).

(B) *De novo* lipogenesis of control and CPT2$^{A-/-}$ MEFs from ^{3}H-Acetate or 2-^{14}C-Pyruvate normalized to protein concentration. (n=6).

(F) Substrate oxidation of control and CPT2$^{A-/-}$ MEFs from 2-^{14}C-Pyruvate or U-^{14}C-Glucose normalized to protein concentration. (n=5). Data are expressed as means +/− SEM. *p<0.05. Open bars represent control and black bars represent loss of CPT2.

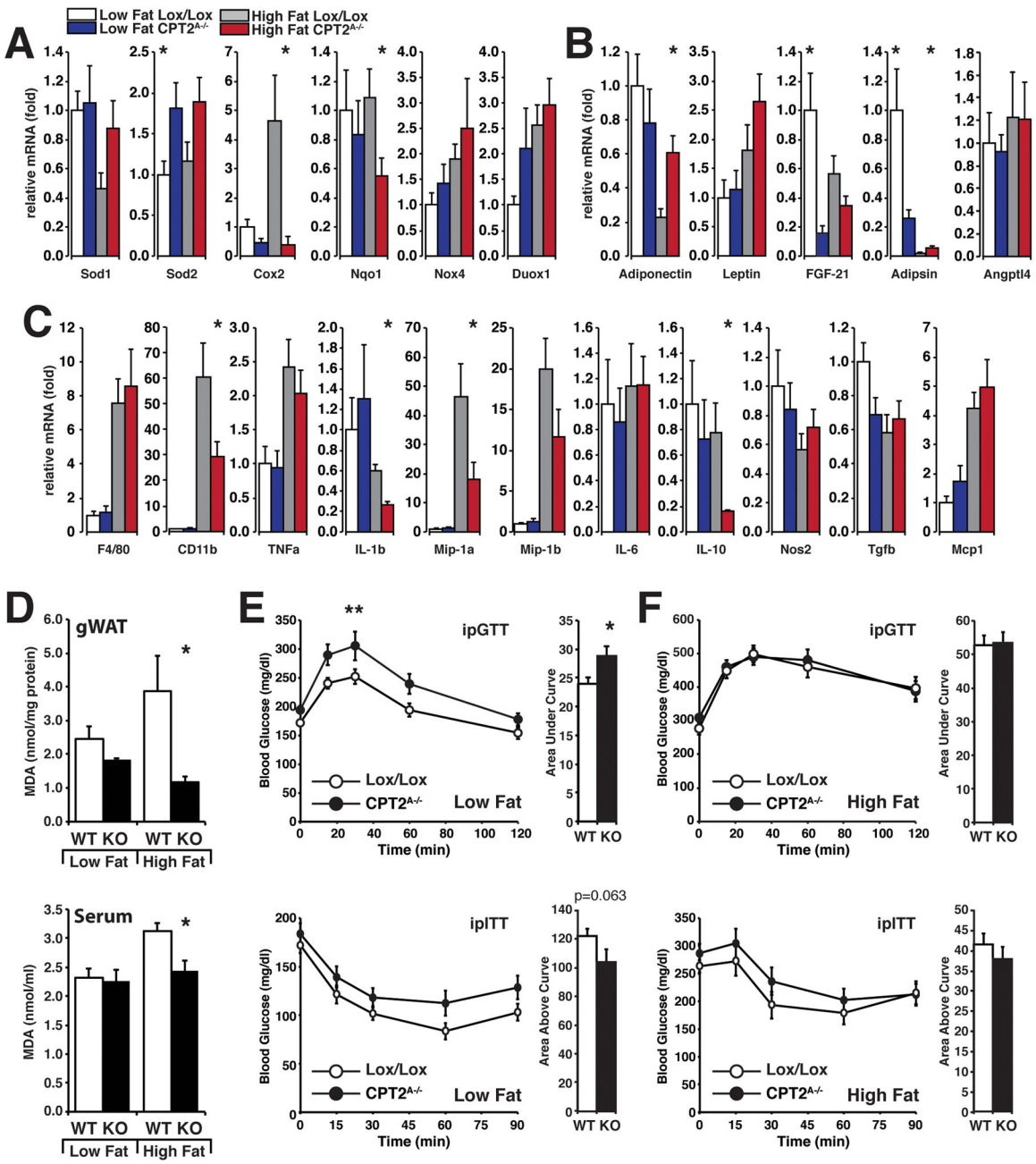

Figure 7. Adipose fatty acid oxidation potentiates high fat induced oxidative stress and inflammation

(A) qRT-PCR of oxidative stress genes from gWAT of control and CPT2$^{A-/-}$ mice fed low or high fat diets (n=8).

(B) qRT-PCR of adipokines from gWAT of control and CPT2$^{A-/-}$ mice fed low or high fat diets (n=8).

(C) qRT-PCR of inflammatory genes from gWAT of control and CPT2$^{A-/-}$ mice fed low or high fat diets (n=8).

(D) TBARS assay from gWAT and serum of control and CPT2$^{A-/-}$ mice fed low or high fat diets (n=5).

(E) ipGTT and ipITT including area under the curve and area above the curve, respectively for control and CPT2$^{A-/-}$ mice fed a low fat diet (n=9).

(F) ipGTT and ipITT including area under the curve and area above the curve, respectively for control and CPT2$^{A-/-}$ mice fed a high fat diet (n=13–18). Data are expressed as means +/− SEM. **p<0.005, *p<0.05